Biochimica et Biophysica Acta 1842 (2014) 1707–1719

Contents lists available at ScienceDirect

Biochimica et Biophysica Acta

journal homepage: www.elsevier.com/locate/bbadis

PACAP27 prevents Parkinson-like neuronal loss and motor deficits but not microglia activation induced by prostaglandin J2

Kai-Yvonne Shivers [a], Anastasia Nikolopoulou [b], Saima Ishaq Machlovi [a], Shankar Vallabhajosula [b], Maria E. Figueiredo-Pereira [a,*]

[a] Department of Biological Sciences, Hunter College, Graduate School and University Center, CUNY, New York, NY 10065, USA
[b] Department of Radiology, Citigroup Biomedical Imaging Center, Weill Cornell Medical College of Cornell University, New York, NY 10065, USA

ARTICLE INFO

Article history:
Received 15 March 2014
Received in revised form 11 June 2014
Accepted 17 June 2014
Available online 23 June 2014

Keywords:
Prostaglandin J2
PET
Microglia
PACAP
Parkinson
PK11195

ABSTRACT

Neuroinflammation is a major risk factor in Parkinson's disease (PD). Alternative approaches are needed to treat inflammation, as anti-inflammatory drugs such as NSAIDs that inhibit cyclooxygenase-2 (COX-2) can produce devastating side effects, including heart attack and stroke. New therapeutic strategies that target factors downstream of COX-2, such as prostaglandin J2 (PGJ2), hold tremendous promise because they will not alter the homeostatic balance offered by COX-2 derived prostanoids. In the current studies, we report that repeated microinfusion of PGJ2 into the *substantia nigra* of non-transgenic mice, induces three stages of pathology that mimic the slow-onset cellular and behavioral pathology of PD: mild (one injection) when only motor deficits are detectable, intermediate (two injections) when neuronal and motor deficits as well as microglia activation are detectable, and severe (four injections) when dopaminergic neuronal loss is massive accompanied by microglia activation and motor deficits. Microglia activation was evaluated in vivo by positron emission tomography (PET) with [^{11}C](R)PK11195 to provide a regional estimation of brain inflammation. PACAP27 reduced dopaminergic neuronal loss and motor deficits induced by PGJ2, without preventing microglia activation. The latter could be problematic in that persistent microglia activation can exert long-term deleterious effects on neurons and behavior. In conclusion, this PGJ2-induced mouse model that mimics in part chronic inflammation, exhibits slow-onset PD-like pathology and is optimal for testing diagnostic tools such as PET, as well as therapies designed to target the integrated signaling across neurons and microglia, to fully benefit patients with PD.

1. Introduction

Neuroinflammation, particularly microglia and astrocytes, play a critical role in the pathogenesis of Parkinson's disease (PD) [19,22,55,84]. A critical factor of neuroinflammation is cyclooxygenase-2 (COX-2), which is highly induced in PD and negatively impacts neuronal function [7,25,40,85]. COX-2 is a key enzyme in the biosynthesis of prostaglandins, some of which are neuroprotective while others are neurotoxic [36]. The role of prostaglandins in PD pathology is poorly defined. In the previous studies we compared in vitro the neurotoxic effects of four different prostaglandins, i.e. A1, D2, E2, and J2, and established that prostaglandin J2 (PGJ2) was the most neurotoxic at the concentrations tested [47].

PGJ2 is derived from PGD2 [87], the principle cyclooxygenase product synthesized in the mammalian CNS [1,14,30]. From all prostaglandins, PGD2 levels change the most under pathological conditions [26,48]. PGD2 readily undergoes non-enzymatic dehydration to generate PGJ2, which is unique among prostaglandins as it is highly reactive and forms covalent Michael adducts with cellular proteins [87].

The levels of PGJ2 in the brain are highly elevated in rodent models of stroke [50,51] and traumatic brain injury (TBI) [31,45], reaching the 100 nM range. These levels represent average brain concentrations, but it is predicted that local cellular and intracellular concentrations of PGJ2 could be much higher [52]. Importantly, stroke and TBI increase the long-term risk for PD [8,35,73,86]. Moreover, PGJ2 impairs the ubiquitin/proteasome pathway (UPP) [41,47,76,90] and mitochondrial function [42,43,54], and potentiates dopamine toxicity [64]. Based on all of these findings we propose that PGJ2 plays an important role in PD pathogenesis. In effect, we showed that microinfusing PGJ2 alone

Abbreviations: COX-2, cyclooxygenase-2; DA, dopamine; DMSO, dimethyl sulfoxide; MPTP, 1-Methyl 4-phenyl 1,2,3,6-tetrahydropyridine; 6-OHDA, 6-Hydroxydopamine; PD, Parkinson's disease; PBS, phosphate buffered saline; PACAP, pituitary adenylate cyclase-activating polypeptide; PGD2 and J2, prostaglandin D2 and J2: respectively; PD, Parkinson's disease; PET, positron emission tomography; SEM, standard error of the mean; SNpc and SNpr, *Substantia nigra pars compacta and pars reticulata*: respectively; TBI, traumatic brain injury; TH, tyrosine hydroxylase; Ub-protein, ubiquitinated protein; UPP, ubiquitin/proteasome pathway; VTA, ventral tegumental area

* Corresponding author at: Department of Biological Sciences, Hunter College, CUNY, 695 Park Avenue, Room 827N, New York, NY 10065, USA. Tel.: +1 212 650 3565; fax: +1 212 772 5227.
E-mail address: pereira@genectr.hunter.cuny.edu (M.E. Figueiredo-Pereira).

http://dx.doi.org/10.1016/j.bbadis.2014.06.020
0925-4439/

into the *substantia nigra/striatum* of mice is sufficient to induce molecular, cellular and behavioral deficits similar to those in PD [69].

To overcome the neurotoxic effects of PGJ2 we tested the impact of the pituitary adenylate cyclase-activating polypeptide (PACAP). PACAP is a potent neuroprotective lipophilic peptide in different models of neuronal injury such as stroke, Parkinson's disease, Huntington's disease, traumatic nerve injury, retinal degeneration, and others, where it exhibits anti-apoptotic, anti-inflammatory and anti-oxidant effects [4,18,53,66,72]. In addition, we previously established that PACAP prevents neuronal death, proteasome deficits and the decrease in cAMP levels induced by PGJ2 in vitro [57]. PACAP signals survival via the activation of the G-protein coupled receptor PAC1R (pituitary adenylate cyclase 1 receptor), which is expressed in the substantia nigra pars compacta (SNpc), in the ventral tegmental area (VTA), and other brain areas [38,81]. Nanomolar concentrations of the two forms of PACAP, PACAP38 and the truncated form PACAP27 (the latter used in our experiments), activate adenylate cyclase and elevate intracellular cAMP [60]. PACAP was shown to mitigate 6-OHDA and MPTP-induced loss of dopaminergic neurons in animal models of PD [17,71,72,89]. Furthermore, PACAP deficiency sensitizes dopaminergic neurons to paraquat-induced neuroinflammation in vivo [92]. Some studies support the view that PACAP27 is a more potent neuropeptide than PACAP38 and VIP (vasoactive intestinal peptide) in, for example, voltage clamped preparations of rat jejunum [15]. Together, these findings support our investigation on the efficacy of PACAP27 against the neurodegenerative effects of PGJ2 with our in vivo model of PD.

Our current study extends our previous one [69], in that we establish progressive stages of pathology induced by four consecutive PGJ2 microinfusions one week apart. These three stages mimic the slow-onset cellular and behavioral deficits in PD: mild (upon one injection) when only slight motor deficits are evident, intermediate (upon two injections) when neuronal and motor deficits as well as microglia activation are significantly detectable, and severe (upon four injections) when dopaminergic neuronal loss is massive accompanied by microglia activation and motor deficits. We also show that PET imaging of the brain with [^{11}C](R)PK11195 qualitatively detects microglia activation induced by PGJ2. Finally, we establish that in the intermediate stage, PACAP27 protects against neuronal loss and motor deficits, but not in the severe stage, which most likely coincides with a point of no return. PACAP27 failed to prevent microglia activation in this rodent model of PD-like pathology. It is clear that brain injury, initiated in our model by a neurotoxic product of inflammation, involves integrated signaling across neurons and microglia. Ideally, therapeutic interventions for PD should target all cells involved regardless of cell type, i.e. neurons and glia.

2. Materials and methods

2.1. Materials

Drugs: PGJ2 (cat. # 18500, Cayman Chemical) in DMSO, and PACAP27 (pituitary adenylate cyclase-activating polypeptide, cat. # H-1172, Bachem Bioscience) in sterile water. The final DMSO concentration in PBS was 17% for all microinfusions. The solutions were freshly prepared and stored for a maximum of 2 h at 4 °C and in the dark. *Primary antibodies*: dopaminergic neurons [tyrosine hydroxylase (TH), 1:1000, cat.# MAB318 (mouse) or AB152 (rabbit), Millipore]; GABAergic neurons [GAD67, 1:1,000, cat.# MAB5406 (mouse), Millipore]; all neurons [NeuN, 1:50, cat.# MAB377 (mouse), Millipore]; microglia and macrophages [Iba1, 1:500, cat.# 019-19741 (rabbit), Wako Chemicals]; and ubiquitinated proteins [1:200, cat.# Z0458 (rabbit), Dako Cytomation]. *Secondary antibodies*: Alexa Fluor 568 (1:100, cat.# A11036, rabbit) and Alexa Fluor 488 (1:100, cat.# A11029, mouse) both from Invitrogen. Vectashield Hard Set™ mounting medium with DAPI (cat.# H-1500, Vector Laboratories).

2.2. Mice

Eleven-week old male FVB mice (N = 43; body weight: 25–32 g) were obtained from Charles River. Mice were singly housed on a 12-h light/dark cycle, maintained at 23 °C and 50–70% humidity, with food and water available ad libitum. Mice were allowed to acclimate for two weeks before surgery. All procedures were performed in accordance with the NIH Guidelines for the Care and Use of Laboratory Animals and were approved by the Institutional Animal Care and Use Committees at Hunter College, CUNY and at Weill Cornell Medical College.

2.3. Surgery and microinfusion

We followed the same procedures as described in our previous study [69], except that mice received unilateral injections of vehicle (DMSO) or drugs (PGJ2 and PACAP27) only into the SN. Briefly, at thirteen weeks of age, mice were anesthetized by isoflurane inhalation (induction 2–2.5%, maintenance 1.5–2%) administered in 100% oxygen and placed into a stereotaxic frame (Model 51730D, Stoelting Co., Wood Dale, IL) fitted with a gas anesthesia mask (Model 50264, Stoelting Co.). A burr hole was drilled in the skull at coordinates relative to bregma for the SNpc [67]: rostral–caudal (RC) = −3.25 mm; medial–lateral (ML) = 1.25 mm; and ventral = 4.13 mm. All injections were administered to the right SNpc, while the contralateral (left) side served as an internal control. A 2 μL microinjection Hamilton syringe (7002 KH) with a 25-gauge needle was slowly inserted into the brain and left in place for five minutes. Thereafter, 2 μL of solution was infused at an injection rate of 0.2 μL/min (Quintessential stereotaxic injector, Model 53311, Stoelting Co.). The needle was left in place an additional five minutes to ensure total diffusion of the solution. Following injection, the needle was slowly removed and the incision was closed with monofilament absorbable sutures (cat. # 033899; Butler Schein Animal Health, Dublin, OH). After surgery, mice were administered with a subcutaneous injection of 0.5 cc Lactated Ringer's solution, given wet palatable rodent chow, and kept in a warm place to recover. Subsequent injections to the SNpc were administered via the same drill hole established during the first surgical procedure.

2.4. Groups

Mice were randomly assigned to the treatment groups (Fig. 1). For behavioral and immunohistochemical analyses, mice in each group received either two (2×, n = 3) or four (4×, n = 6) injections of DMSO, or either one (1×, n = 7), two (2×, n = 6) or four (4×, n = 6) injections of PGJ2. Moreover, to assess the therapeutic efficacy of PACAP27, other groups of mice received two injections of PACAP27 (2×, n = 3), or two injections of PACAP27 + PGJ2 (2×, n = 3) and were compared to the mice receiving DMSO (2×) or PGJ2 (2×). In preliminary studies we established that PACAP27 (4×) was ineffective against four PGJ2 injections, thus we did not utilize a 4× PACAP treatment group in our current paradigm. Behavior was assessed four weeks after the last microinfusion. Following behavioral assessment, animals were perfused intracardially and the brains removed for immunohistochemical analyses. To obtain maximal signal for μPET imaging, one group of mice (4×, n = 5) received four unilateral DMSO injections and another group (4×, n = 5) received four unilateral PGJ2 injections. Mice underwent μPET scanning one week after the last PGJ2 or DMSO injection. The concentrations per unilateral injection were 16.7 μg/2 μL for PGJ2 and 50 ng/2 μL for PACAP27, administered individually or co-injected. All injections were administered one week apart.

2.5. Behavior

Mice were tested for Parkinsonian-like behavior four weeks after their last injection (Fig. 1). Scorers were blind to the experimental

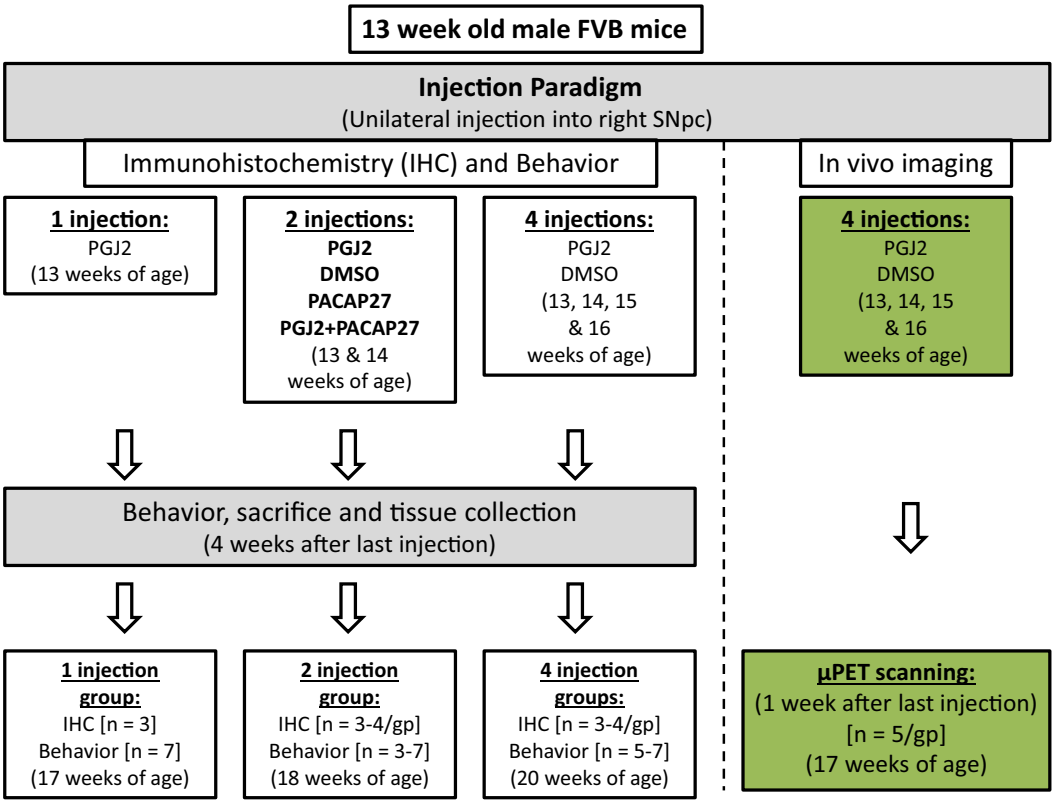

Fig. 1. Schematic representation of the experimental design. Thirteen-week-old male FVB mice were microinjected into the right *substantia nigra pars compacta* (SNpc) as shown. Mice received one, two or four microinfusions of either DMSO (control; 17% in PBS), PGJ2 (16.7 µg), PACAP27 (50 ng), or PGJ2 and PACAP27 in 2 µL DMSO/PBS, at weekly intervals as shown. For all mice motor behavior was assessed four weeks after the last injection. Following behavioral assessment, mice were perfused intracardially and the brains were removed for immunohistochemical analyses. For in vivo imaging, mice that received four (4×) DMSO or PGJ2 injections underwent micro-positron emission tomography (µPET) scanning one week after the last injection. n = number of mice per group (gp).

treatments, and their scores were averaged and statistically analyzed. Inter-scorer reliability was highly correlated (Pearson $r > 0.95$). There are batteries of tests that can be used to study PD-related behavioral changes in rodents [79]. We chose two: 1) *Forelimb use asymmetry* — assessed with the cylinder test as in [75]. This test reliably evaluates spontaneous vertical exploration and limb use asymmetry in a novel environment [56], which is a sensitive behavioral test used to detect unilateral damage to the nigrostriatal pathway [75]. Given the unilateral damage to the SN in our model, we anticipated stronger effects with asymmetry evaluated with the cylinder test, rather than changes in spontaneous movement [12]. Limb use asymmetry was expressed as a ratio of ipsilateral paw over contralateral paw usage and normalized as percent of the respective control. 2) *Curling*: this test is used to assess body axis asymmetry resulting from unilateral damage to the nigrostriatal pathway [29,56,91], and was performed as in our previous study [69]. Curling behavior was averaged per group and expressed as a ratio of curling behavior upon PGJ2 treatment over DMSO treatment.

2.6. Immunohistochemistry

Four weeks after their last microinfusion, mice were terminally anesthetized (i.p.) with ketamine (100 mg/kg) and acepromazine (3 mg/kg), and transcardially perfused with 4% paraformaldehyde in PBS. The mouse brains were removed, post-fixed overnight at 4 °C, followed by cryoprotection (30% sucrose/PBS at 4 °C). Brains were sectioned in the coronal plane using a freezing microtome at a thickness of 30 µm, and sections were collected serially along the rostrocaudal axis of the striatum and *substantia nigra pars compacta* (SNpc) [between 1.54 mm and −0.10 mm for the striatum, and −2.46 mm and −3.88 mm for the SNpc; coordinates relative to bregma, as in [67]. Tissue series (seven series for the striatum and four series for the SNpc) were stored at 4 °C (TBS, pH7.4 plus 0.1% sodium azide) until use. Each series was processed as free floating sections for immunohistochemical analyses as described in [69].

2.7. Stereology

Unbiased stereology analysis was conducted by scorers blind to the experimental treatments. Total number of TH+, NeuN+, and Iba1+ cells were obtained with the Zeiss AxioVision Release 4.8.2 Software unbiased stereology programming (Carl Zeiss Group, Jena, Germany). Sections were viewed on an Axio Imager M2 Zeiss microscope (Carl Zeiss Group) equipped with a motorized stage and a high resolution AxioCam MRm Rev. 3 camera (Carl Zeiss Group). The outline of the SNpc delineated by TH + staining [6] was obtained at low (5×) magnification, and sampling of 10 sites per section with the optional fractionator probe, were averaged. Eight SNpc sections spaced 120 µm apart were used for the analyses. Cells were counted at 63× along the rostrocaudal axis, and at predetermined intervals [x-step = 175 µm; y-step = 175 µm; 30,625 μm^2; frame associated area (grid size): horizontal = 113.497 µm, vertical = 85.071 µm; 9655.322 μm^2]. The z-dimension was defined as 20 µm, thus providing a 5 µm guard on the top and bottom surface of each section, for error due to tissue damage. AxioVision Rel. 4.8 Gundersen coefficients of error were less than or equal to 0.1. Values obtained were an estimate of cell numbers in the whole *substantia nigra*. Dopaminergic (DA) cell counts from the intact SNpc were similar to a previous report [63]. Care was taken to ensure that cells within the ventral tegmental area (VTA) were excluded from SN quantification.

2.8. Mosaic image acquisition and striatum analysis

Mosaic images for the SN and striatum were captured with the AxioVision 4 module MosaiX software, using a Zeiss AxioCam MRm Rev. camera connected to a motorized stage. A range of 16–24 tiled images for the SN and 24–30 images for the striatum was captured at 5×, combined and converted into a TIFF file.

Densitometry (optical density, O.D.) of the TIFF mosaic images representing the TH + terminals in the contralateral and ipsilateral dorsal striatum was performed with the ImageJ software (ImageJ, Rasband, W.S., ImageJ, U.S. NIH, Maryland, http://rsb.info.nih.gov/ij/, 1997–2006) as described in [27]. The striatum was divided along the dorsoventral axis to obtain values specific for the dorsal striatum, the main region of the striatum innervated by dopaminergic terminals projecting from the SNpc [27]. Three tissue analyses per treatment group were used for quantification. Nonspecific background density was corrected for by subtracting out completely denervated areas surrounding the striatum. Data was expressed as O. D. from the ipsilateral dorsal striatum divided by the contralateral, and normalized as percent to DMSO control.

2.9. Micro-positron emission tomography (μPET) imaging

μPET imaging was performed using the Inveon trimodal system (Siemens Medical Solutions USA) with a transaxial FOV of approximately 10 cm and an axial FOV of 12.7 cm. [^{11}C](R)PK11195 was synthesized at the Citigroup Biomedical Imaging Center of Weill Cornell Medical College following a published procedure [5]. The radiochemical purity of the final product was >98% with a specific activity of >13 Ci/μmol. The dose for imaging the mice ranged from 10 to 30 MBq. Mice were given a tail vein injection of [^{11}C](R)PK11195 (as a solution of 150–250 μL saline). Subsequently, mice were anesthetized with isoflurane (2–3% in oxygen) and imaging was started at 30 min after the radiotracer administration. PET scans were acquired for 20 min followed by a 10 min CT scan. [^{11}C](R)PK11195-PET imaging studies were performed in PGJ2-treated and DMSO-treated mice one week after the last treatment.

Analysis of the imaging data was performed using the Inveon Research Workstation (IRW) software (Siemens Medical Solutions). Images were reconstructed using OSEM3D (2 iterations and 16 subsets), with a voxel size of 0.78 mm × 0.78 mm × 0.80 mm. Regions of Interest (ROIs) were defined on summed PET images and Volumes of Interest (VOIs) were placed on both right and left *substantia nigra* (SN) and cerebral cortex. Tracer uptake in each VOI was estimated as nanocuries/cubic centimeters (nCi/cc). Two tracer uptake ratios were determined: (1) SN lesion (ipsilateral side)/contralateral (intact) SN, and (2) SN lesion (ipsilateral side)/contralateral cerebral cortex.

2.10. Statistical analyses

All data are expressed as the mean ± SEM. Statistical analyses were performed with GraphPad Prism 6 (GraphPad Software, San Diego, CA). A p-value < 0.05 was considered statistically significant. For group comparisons, we performed one-way analysis of variance (ANOVA) followed by *post hoc* Tukey's test for multiple comparison. Correlations between two variables were evaluated by linear regression calculating the Pearson correlation coefficients. [^{11}C](R)PK11195 radiotracer uptake analyses were performed with Student's t test.

3. Results

3.1. Slow-onset dopaminergic neuronal loss in the SNpc/striatum induced by PGJ2

Using our recently established model of PD-like pathology, we investigated in vivo the gradual effects of subchronic inflammation. For this purpose, mice were administered unilateral (right side) injections of 16.7 μg/2 μL PGJ2 to the SNpc for one, two or four weeks (once per week) as depicted in Fig. 1. Our data show that increasing the weeks of exposure to PGJ2 progressively intensified the dopaminergic (DA) neuronal loss in the SNpc (Fig. 2A and C). The contralateral SNpc served as the uninjected control. To assess DA specific damage (Fig. 2A, B and C) we performed immunohistochemical (IHC) staining for tyrosine hydroxylase (TH) and for neuron-specific nuclear protein (NeuN). It is clear that a single injection of PGJ2 produced no IHC detectable changes in DA neurons (Fig. 2A, B and C). However, two and four injections of PGJ2 led to a significant decline in DA (TH+) neurons in the SNpc, by 33.4% and 58.7% respectively, compared to DMSO control. The decline in SNpc DA neurons upon four injections of PGJ2 was significantly greater than that induced by two PGJ2 injections ($p < 0.05$) supporting the gradual nature of the PGJ2-induced neuronal loss. No significant differences in TH staining were detected in the contralateral SNpc in any groups tested ($F_{(3, 8)} = 0.78$, $p = 0.54$; Fig. 2A and C). Under all experimental conditions, the DA neurons in the VTA were spared or minimally affected (Fig. 2A).

As shown in Fig. 2C, NeuN + immunoreactivity decreased significantly following PGJ2 administration [$F_{(4, 11)}$ 20.87, $p = 0.0001$], thus corroborating that the loss in TH immunostaining was due to the degeneration of DA neurons and not to TH depletion (Fig. 2B and C).

With four injections of PGJ2 the damage from the SNpc spread to the striatum, depicted by the decline in TH positive staining (Fig. 3). Optical density (O.D.) analysis of TH + terminals at the dorsal striatum showed that four injections of PGJ2 led to a significant TH + terminal loss as compared to all other conditions [$F_{(3, 8)} = 17.19$, $p = 0.0008$, Fig. 3A and B]. Pearson correlation coefficients indicate a significant positive correlation between the number of ipsilateral TH + cells in the SNpc and TH + O.D. in the dorsal striatum ($r^2 = 0.69$, $p = 0.0009$; Fig. 3C). This analysis supports a positive correlation between the loss of TH staining in the ipsilateral SNpc and TH terminal loss in the dorsal striatum upon PGJ2 administration.

3.2. Accumulation of ubiquitinated proteins induced by PGJ2 microinfusion

One of the hallmarks of PD is the accumulation/aggregation of ubiquitinated proteins in Lewy bodies [21]. This aspect of PD was addressed in our study. We established that compared to DMSO, microinfusion of PGJ2 increased the levels of aggregate-like ubiquitin conjugates in the DA neurons of the SNpc (Fig. 4A and B). More DA neurons exhibiting increased levels of ubiquitinated proteins were detected in the SNpc of mice that received two than four PGJ2 injections, because more DA neurons survived in the former mice. Fig. 4B shows the distribution of the aggregate-like ubiquitin conjugates under high magnification, in mice injected 4× with PGJ2.

3.3. PGJ2 administration increases microglia activation in the SNpc

The rise in activated microglia due to PGJ2 administration was statistically significant ($F_{(4, 12)} = 9.55$, $p = 0.001$), as detected by immunostaining for Iba1 (Fig. 5A and B). The number of activated microglia in the SNpc was initially ~1800 (uninjected, contralateral side) and increased gradually, parallel to the number of PGJ2 injections, reaching more than 7000 upon four PGJ2 injections. The increase in activated microglia was significant upon two and four PGJ2 injections (at least $p < 0.01$; Fig. 5B). In addition, there was a significant negative correlation between TH + and Iba1 + cell numbers in the ipsilateral SNpc ($r^2 = 0.35$, $p = 0.043$, Fig. 5C). Due to the surgical procedure, intranigral injection of DMSO alone also increased microglia activity and so did one PGJ2 injection, but these changes did not reach statistical significance as compared to the contralateral SNpc (Fig. 5B).

A major hallmark of microglial activation is the expression of the peripheral benzodiazepine receptor, also known as the translocator protein TSPO [13]. The levels of TSPO are very low in the brain, and

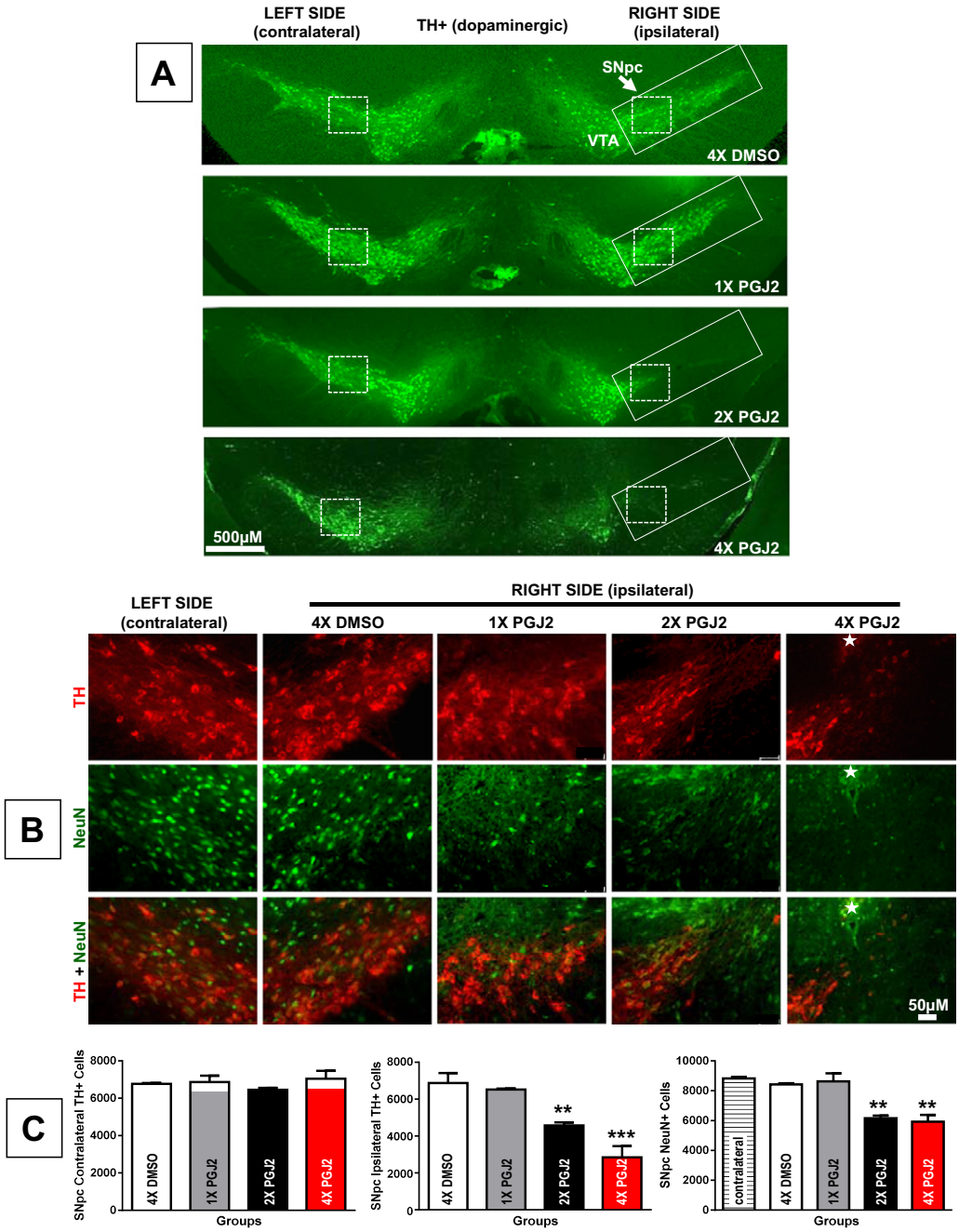

Fig. 2. Dopaminergic neuronal loss in the ventral midbrain upon successive intranigral PGJ2 lesions. A — Representative coronal sections of the ventral midbrain depicting dopaminergic neurons. TH-immunoreactivity was strong in the VTA (ventral tegmental area) and SNpc (*substantia nigra pars compacta*, rectangle) of control (DMSO) mice and those receiving one PGJ2 injection (1× PGJ2). TH-immunoreactivity decreased in a gradual manner in the ipsilateral SNpc of mice receiving two (2×) or four (4×) PGJ2 injections. Dopaminergic neurons in the VTA were spared. No significant differences in TH + were observed in the contralateral SNpc of the different groups of mice. Scale bar = 500 μm. Inset: All magnified images shown in B were captured at the representative region of the SNpc indicated by the dashed square boxes. B — TH (*red*, dopaminergic neurons) and NeuN (*green*, all neurons) immunostaining of the SN shows a gradual loss of dopaminergic neurons in the ipsilateral SNpc after two (2×) and four (4×) microinjections of PGJ2. No dopaminergic neuronal loss was observed in the contralateral side nor in the ipsilateral side of DMSO or 1× PGJ2-injected mice. The star indicates the site of injection. Scale bar = 50 μm. C — The extent of PGJ2 lesion was assessed by calculating the total number of TH + or NeuN + neurons (mean ± SEM) in the SNpc using unbiased stereology as described in Materials and methods. The asterisk (*) identifies the values that are significantly different from DMSO-injected mice: **, $p < 0.01$; ***, $p < 0.001$. $N = 3$ to 4 mice per group.

increase dramatically upon microglia activation following brain injury [13]. The isoquinoline carboxamide PK11195 is selective for TSPO and displays nanomolar binding affinity, thus being ideal for imaging microglia activation [5]. To obtain a regional estimation of brain inflammation in vivo, we evaluated microglia activation in the mice by performing micro positron emission tomography (μPET) with the radioligand [^{11}C](R)PK11195. To obtain maximal signal, μPET sessions were performed one week following four DMSO or PGJ2 injections.

The brain distribution and uptake of [^{11}C](R)PK11195 in the PGJ2 and DMSO treated mice based on imaging studies, are depicted in Fig. 5D. The data in the graphs are presented as two tracer uptake ratios: top graph – ipsilateral (injected) SN/contralateral (intact) SN; bottom graph – ipsilateral (injected) SN/contralateral cerebral cortex (Ctx). It is clear that [^{11}C](R)PK11195 uptake was qualitatively more pronounced in PGJ2 than in DMSO-injected mice confirming that PGJ2 induces microglia activation. The tracer uptake trend was consistent for the ipsilateral SN/contralateral SN ratio: 2.31 ± 0.32 for PGJ2-treated

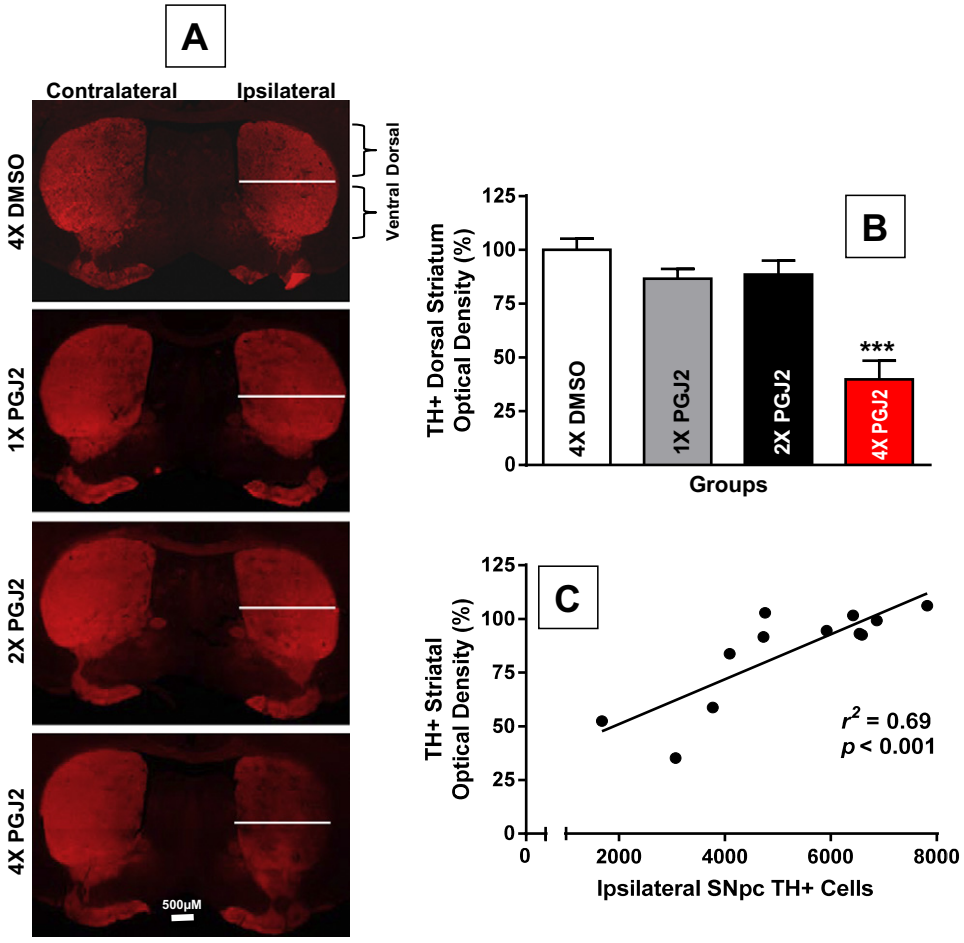

Fig. 3. Extent of dopaminergic degeneration in the striatum upon successive intranigral PGJ2 lesions. A — Representative coronal sections of the striatum depicting TH-innervation. The white line on the ipsilateral side separates dorsal and ventral striatum. A prominent loss of TH + innervation (*red*) was observed in the ipsilateral dorsal striatum of mice treated with four (4×) PGJ2 injections as compared to all other treatments. Scale bar = 500 μm. B — The extent of the loss of TH + innervation is expressed as optical density in the dorsal striatum. The asterisk (*) identifies the values that are significantly different from all other groups: ***, $p < 0.001$. $N = 3$ to 4 mice per group. C — In the PGJ2-treated mice, dopaminergic cell loss (Th+) in the ipsilateral SNpc (y-axis) directly correlates with the loss of TH + innervation (optical density) in the ipsilateral dorsal striatum (x-axis). The extent of PGJ2 lesion was assessed by calculating the number of TH + cells in the SNpc using unbiased stereology, while the TH + innervation in the dorsal striatum was measured using semi-quantitative densitometry as described in Materials and methods.

mice versus 1.68 ± 0.13 for DMSO-treated mice (Fig. 5D, top graph), and for the ipsilateral SN/contralateral Ctx ratio: 1.76 ± 0.14 for PGJ2-treated mice versus 1.42 ± 0.11 for DMSO-treated mice (Fig. 5D, bottom graph). However, in both cases the difference between the two groups (DMSO and PGJ2-treated) failed to reach statistical significance ($p = 0.11$, top graph; $p = 0.08$, bottom graph). We followed microglia activation at 9 weeks after the fourth injection, and the difference between PGJ2 treatment compared to DMSO was still evident (ipsilateral SN/contralateral SN ratio: $p = 0.06$; ipsilateral SN/contralateral Ctx ratio: $p = 0.09$, studies in progress).

3.4. PGJ2 injected mice gradually develop Parkinsonian-like motor deficits

Clinically, PD is characterized by the presence of motor deficits caused by the loss of dopamine from dysfunctional dopaminergic neurons in the *substantia nigra* [9,23,33]. To establish the effect of PGJ2 administration on motor performance we used two behavioral tests: the cylinder test which assesses limb use asymmetry, i.e. the rodent's preference for using the ipsilateral over the contralateral paw (Fig. 6A), and the curling test which establishes postural instability (Fig. 6B). The results demonstrate that injection of even a single dose of PGJ2, upon which there are no statistically significant changes in DA neurons (Fig. 2B and C), results in behavioral abnormalities when comparing PGJ2 and DMSO groups (Fig. 6A and B).

Weekly PGJ2 administration induced a gradual and significant bias toward use of the ipsilateral over the contralateral paw ($F_{(3, 21)} = 7.79$, $p = 0.0011$; Fig. 6A), and postural instability consistent with a unilateral lesion ($F_{(3, 19)} = 38.47$, $p = 0.0001$; Fig. 6B). Pearson correlation coefficients indicate a significant negative correlation between ipsilateral paw use and the number of ipsilateral TH + cells in the SNpc ($r^2 = 0.34$, $p = 0.048$; Fig. 6C), as well as a negative trend between ipsilateral paw use and TH + O.D. in the dorsal striatum ($r^2 = 0.26$, $p = 0.13$; Fig. 6D). To address the effects of PGJ2 on spontaneous vertical exploration, we tested if PGJ2 altered rearing behavior in the mice, but no significant differences in free rears were observed ($F_{(3, 21)} = 0.59$, $p = 0.63$, *data not shown*).

3.5. PACAP27 prevents dopaminergic neuronal loss and motor deficits induced by PGJ2

Activating cAMP signaling is known to be neuroprotective [78] and to have a positive effect on the UPP [34], which in contrast is inhibited by PGJ2 [41,47,76,90]. Therefore, we explored if increasing intracellular cAMP with PACAP27 would prevent neuronal loss induced by PGJ2. We chose to co-administer the two drugs, as we recently demonstrated in vitro that when combined with PACAP27, PGJ2 retains its full biological activity toward the accumulation of ubiquitinated proteins in cortical neuronal cultures [52]. Thus the two drugs in concentrated

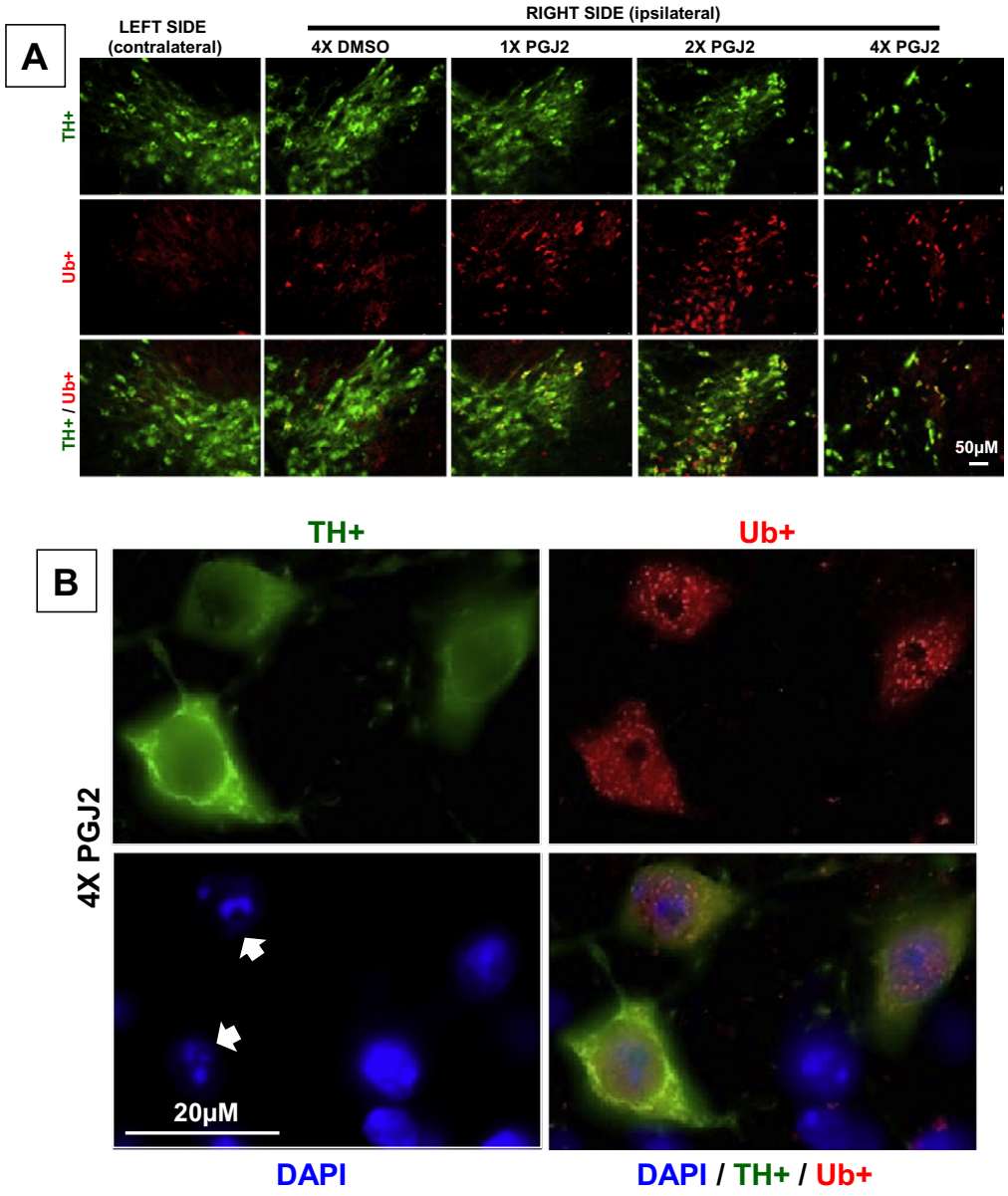

Fig. 4. Successive PGJ2 infusion induces the accumulation/aggregation of ubiquitinated proteins in the dopaminergic neurons. A — Immunostaining for ubiquitinated proteins (Ub; *red*) and TH-positive neurons (*green*) four weeks after the last PGJ2 microinjection. Note the gradual decline in TH + neurons in the ipsilateral SNpc of PGJ2-treated mice. B — Dopaminergic neurons in the SNpc of 4× PGJ2-treated mice exhibit aggregate-like ubiquitin conjugates. Nuclei (DAPI staining) in these neurons exhibit an apoptotic morphology, i.e. a fragmented and/or condensed appearance (*arrows*). Scale bar = 50 μm in A and 20 μm in B.

solutions do not combine to form inactive complexes. In pilot studies we established that PACAP27 was not protective in mice receiving four PGJ2 injections. We thus investigated the neuroprotective effects of PACAP27 in mice that received two PGJ2 injections. It is clear that co-administration of PGJ2 (16.7 μg) and PACAP27 (50 ng) significantly reduced DA neuronal loss in the SN (Fig. 7A, B and C). In PGJ2-treated mice, the number of DA neurons in the ipsilateral SNpc declined significantly compared to those in DMSO or PACAP27 injected mice, or in the contralateral (intact) SNpc ($F_{(4,\ 12)} = 7.76$; $p = 0.003$; Fig. 7B). Co-administration of PGJ2 and PACAP27 prevented the loss of DA neurons induced by PGJ2 ($p < 0.05$; Fig. 7B). Moreover, there was no statistical difference between the number of DA neurons in the contralateral SNpc and in the ipsilateral SNpc of DMSO, PACAP27 or PGJ2 + PACAP27 injected mice, further supporting the neuroprotective effect of PACAP27. Similar results were obtained with NeuN staining (Fig. 7C). PGJ2 caused a significant decrease in NeuN + neurons in the ipsilateral SNpc when compared to all control groups as well as to mice co-treated with PGJ2 + PACAP27 ($F_{(4,\ 11)} = 48.37$, $p = 0.0001$; Fig. 7C). In conclusion, PACAP27 prevents the loss of DA neurons induced by PGJ2 administration in vivo. In contrast, GABAergic neurons in the SNpr region were not affected by PGJ2 microinfusion (Fig. 7A).

The immunohistochemical and behavioral analyses are in agreement. Forelimb use asymmetry and posture stability assessed with the cylinder test and curling test respectively, were significantly altered by PGJ2 ($F_{(2,\ 12)} = 4.52$; $p = 0.035$, for forelimb use asymmetry; $F_{(2,\ 9)} = 61.94$; $p = 0.0001$, for postural stability). Two injections of PGJ2 significantly increased ipsilateral forelimb usage (Fig. 7D, $p < 0.05$) and posture instability (Fig. 7E, $p < 0.001$), as compared to the controls. Co-treatment with PACAP27 prevented the PGJ2-induced motor deficits (Fig. 7E, $p < 0.001$) to the point that there was no significant difference between control and PGJ2 + PACAP27 treated mice. DMSO and PACAP27 treated mice exhibited similar behaviors (*data not shown*) and thus were combined for behavioral analyses and considered as the control group.

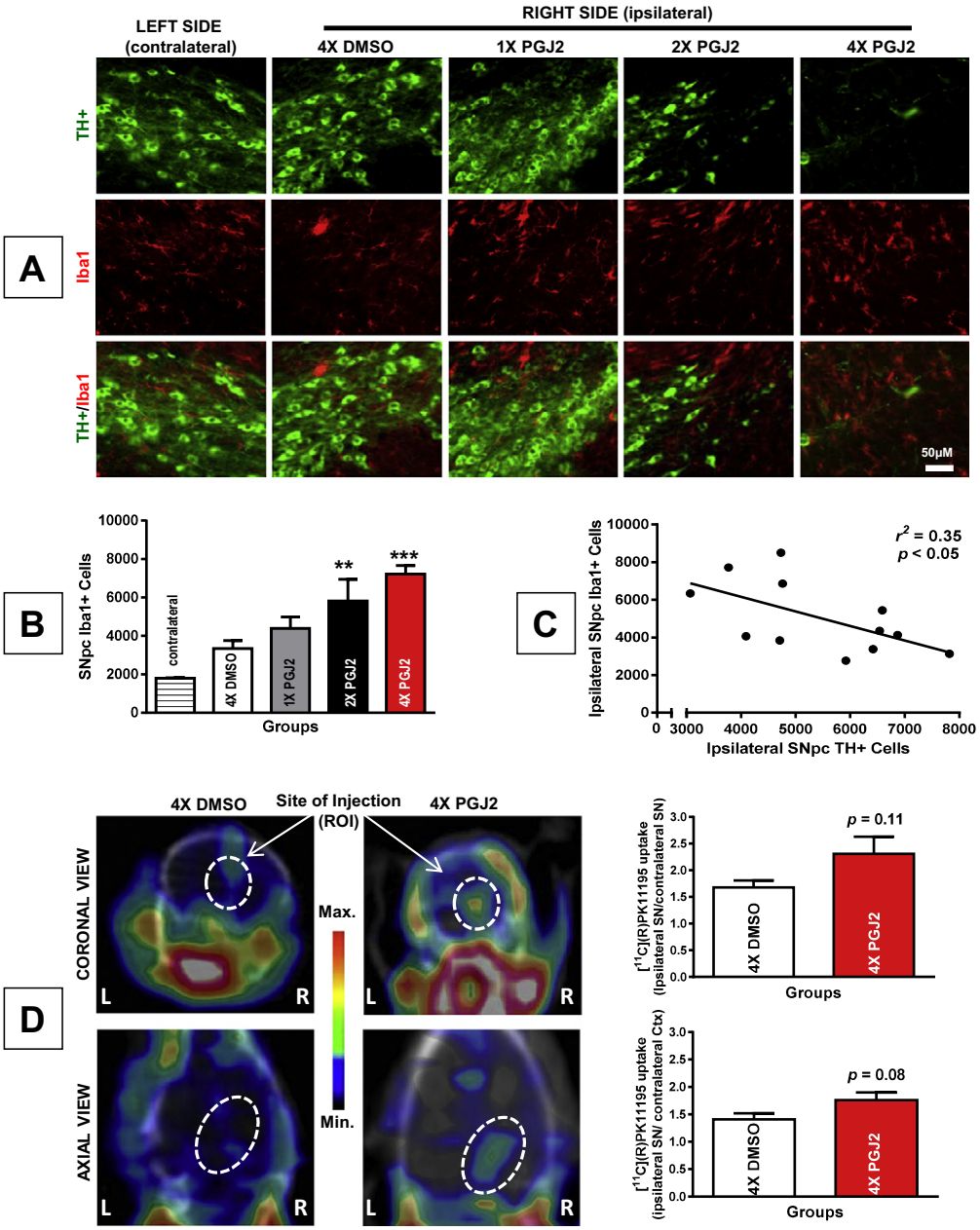

Fig. 5. Successive PGJ2 microinfusion induces microglia activation detected post-mortem and in vivo. A — TH (*green*, dopaminergic) and Iba1 (*red*, activated microglia) immunostaining shows a gradual loss of dopaminergic neurons and gain of activated microglia in the ipsilateral SN of mice receiving two (2×) or four (4×) PGJ2 injections. No difference was apparent between DMSO and 1× PGJ2-treated mice. Scale bar = 50 μm. B — The total number of Iba1+ cells in the SNpc was assessed with unbiased stereology as described in Materials and methods. The asterisk (*) identifies the values that are significantly different from the contralateral SNpc: **, $p < 0.01$; ***, $p < 0.001$. $N = 3$ to 4 mice per group. C — In the ipsilateral SNpc of PGJ2-treated mice, dopaminergic cell loss (TH+, x-axis) negatively correlates with microglia activation (Iba1+, y-axis). D — Using the [^{11}C](R)PK11195 radiotracer, μPET images were taken from 4× DMSO-treated (left panels) and 4× PGJ2-treated (right panels) mice one week after the last injection. Coronal (upper panels) and axial (bottom panels) representative μPET/CT images taken at the level of the SN lesion are shown. A qualitative increase in [^{11}C](R)PK11195 binding was detected in PGJ2-treated compared to DMSO-treated mice. L and R, mouse left and right sides, respectively. Graphs represent the brain uptake of [^{11}C](R)PK11195. The ratios of tracer uptake on the Y-axis represent ipsilateral SN/contralateral SN (top graph) or ipsilateral SN/contralateral cerebral cortex (Ctx, bottom graph) for each treatment. The ratios represent the mean ± SEM of five mice per condition. The *p* values established with Student's *t* test are $p = 0.11$ (top graph) and $p = 0.08$ (bottom graph), are not statistically significant.

3.6. PACAP27 does not prevent neuronal accumulation of ubiquitinated proteins nor microglia activation induced by PGJ2

Co-treatment with PACAP27 failed to diminish the accumulation of ubiquitinated proteins (Fig. 8A) as well as microglia activation (Fig. 8B), both of which induced by two PGJ2 injections as seen in Figs. 4A and 5A, respectively. Microglia activation was assessed by immunostaining with Iba1. While PGJ2 administration (2×) increased microglia activation in the ipsilateral SNpc compared to the contralateral SNpc, co-treatment with PACAP27 failed to prevent this PGJ2 effect ($F_{(4, 12)} = 5.26$; $p = 0.01$, $p < 0.05$; Fig. 8B). Furthermore, there was no significant difference between mice that received PGJ2-injections alone and in combination with PACAP27.

The finding that PACAP27 was unable to prevent the accumulation of ubiquitinated proteins and microglia activation induced by PGJ2, further supports that the two drugs do not combine to form inactive complexes.

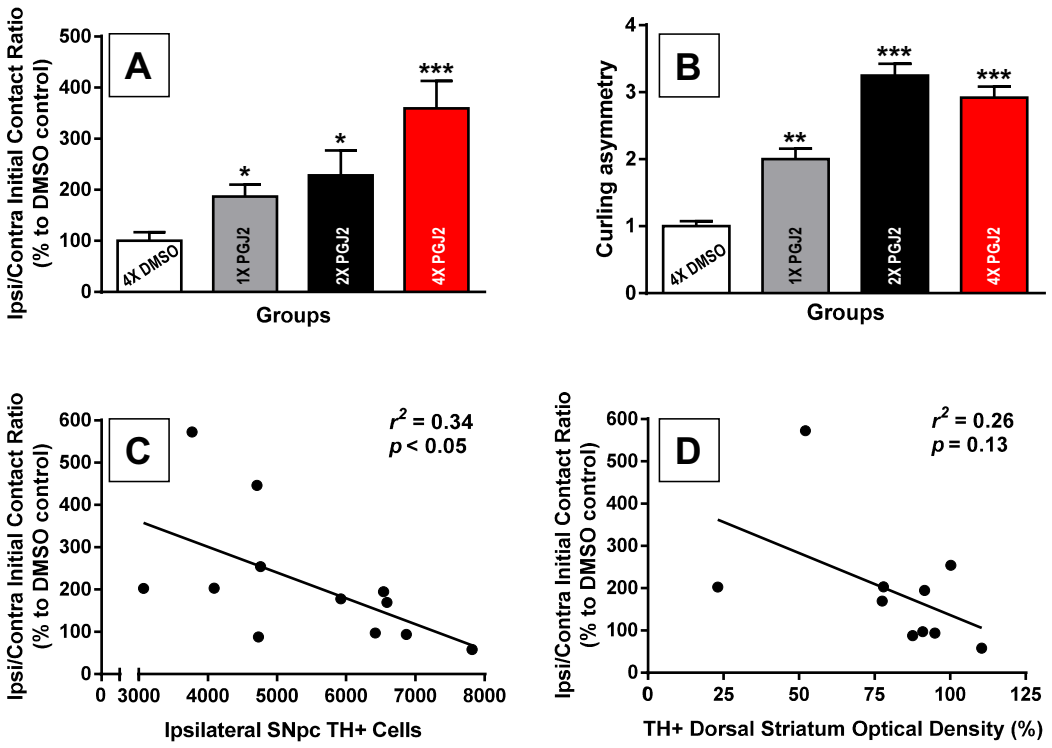

Fig. 6. Correlation of behavioral deficits with the extent of TH + neuronal cell loss in the SN and striatal denervation induced by successive PGJ2 microinfusions. A and B — All groups of mice treated with PGJ2 exhibited behavioral deficits. When compared to DMSO-treated mice, those treated 1×, 2× and 4× with PGJ2 significantly increased usage of the ipsilateral forepaw as measured by the cylinder test (A), and exhibited significant postural instability assessed with the curling test (B) as described in Materials and methods. Statistical significance was estimated with one-way analysis of variance (Tukey–Kramer multiple comparison test) except Student's *t* test was used to compare DMSO vs 1× PGJ2 or vs 2× PGJ2 in (A). The asterisk (*) identifies the values that are significantly different from DMSO-injected mice: *, $p < 0.05$, **, $p < 0.01$; ***, $p < 0.001$. $N = 5$ to 7 mice per group. C and D — In the PGJ2-treated mice, dopaminergic cell loss (TH+) in the ipsilateral SNpc (C), or loss of TH + innervation in the ipsilateral dorsal striatum (D) (both variables represented in the x-axis) inversely correlates with paw usage asymmetry (y-axis). The extent of PGJ2 lesion was assessed by calculating the number of TH + cells in the SNpc using unbiased stereology, while the TH + innervation in the dorsal striatum was measured using semi-quantitative densitometry as described in Materials and methods.

4. Discussion

This study establishes a correlation between successive administrations of PGJ2 to mimic in part chronic inflammation, and progressive DA neuronal loss in the rodent nigrostriatal pathway. As we analyzed the mice upon one, two and four weekly *substantia nigra* microinfusions, we observed that PGJ2 alone was sufficient to induce gradual molecular, cellular and behavioral deficits reminiscent of PD pathology. Therefore, PGJ2 is likely to play an important role in mediating the downstream negative effects of COX-2 in PD. Our previous work established that four microinjections of PGJ2 into the SNpc and striatum of mice led to Parkinsonian-like pathology in a PGJ2-concentration dependent manner [69]. We now show that increasing the number of weeks of exposure to PGJ2 to mimic subchronic inflammation intensifies DA neuronal loss in the SNpc in a parallel manner. Even upon a single injection of PGJ2, when there is no apparent change in neurons assessed by immunostaining for TH and NeuN, there is evidence of SN damage supported by behavioral motor deficits. Increasing the number of PGJ2 injections induced spreading of the damage from the SNpc to the striatum, and gradual microglia activation. Due to its slow-onset, this mouse model extends upon our previous findings by providing an effective means for identifying early molecular mechanisms linked to a particular behavior due to basal ganglia functional deficits. Complete dopaminergic denervation in animal models of PD are particularly well suited for the advanced stages of the disorder when alteration in plasticity [11], loss of striatal dendritic spines [2,16], and changes of glutamatergic signaling [10,68] are identified. However, in the advanced stages of the disease, it is too late to target many of the subtle differences in the disease state that could play a significant role in remediation and in the development of new therapeutics. Understanding the molecular changes underlying the early stages of the disease can be facilitated with the PGJ2-induced mouse model, in which the gradual progression of the disorder can be manipulated and a distinction between behavioral and neuronal deficits is apparent.

The early clinical symptoms of PD are only detected when >70% of DA neurons is already lost [24]; thus more robust detection tools are urgently needed. The close inflammation–neuronal loss relationship yields considerable interest and unmet need for the detection (imaging) and follow-up of neuroinflammation. Positron emission tomography (PET) based on radiopharmaceuticals such as [^{11}C](R)PK11195 that selectively target microglia, the mediators of neuroinflammation, have already shown potential in pre-clinical studies utilizing neuroinflammation induced by toxins such as α-amino-3-hydroxy-5-methyl-4-isoxazolepropionate (AMPA), lipopolysccharide (LPS), 1-methyl-4-phenyl-1,2,3,6-tetrahydropyridine (MPTP), and methamphetamine (METH), and also in some pilot clinical studies [88]. We now show for the first time (to our knowledge) that μPET imaging with [^{11}C](R) PK11195 can be used to qualitatively assess changes in microglia activation in the PGJ2-induced mouse model of PD. Microglia activation is mediated by extrinsic factors (e.g. CD200, CX3CR1, and TREM2) as well as intrinsic factors (e.g.,Runx-1, Irf8, and Pu.1) [39], and astrocytes play an important role in regulating microglia activation [77]. The mechanisms by which PGJ2 induces microglia activation are still unknown. We previously established that PGJ2 increases the levels of the pro-inflammatory cytokine interleukin-1 (IL-1) in neuronal cells [46]. Considering that IL-1 mediates microglia activation in LPS-injected mice [83], it is plausible that the PGJ2-induced microglia activation is, in part, mediated by IL-1. Increases in IL-1 levels are relevant to PD pathogenesis, as its levels are high in the brains of PD patients compared to healthy controls [58], and in PD animal models [44,70].

PGJ2 exerts its action via receptor-mediated and receptor-independent signaling. On the one hand, PGJ2 signals via the G*i* coupled

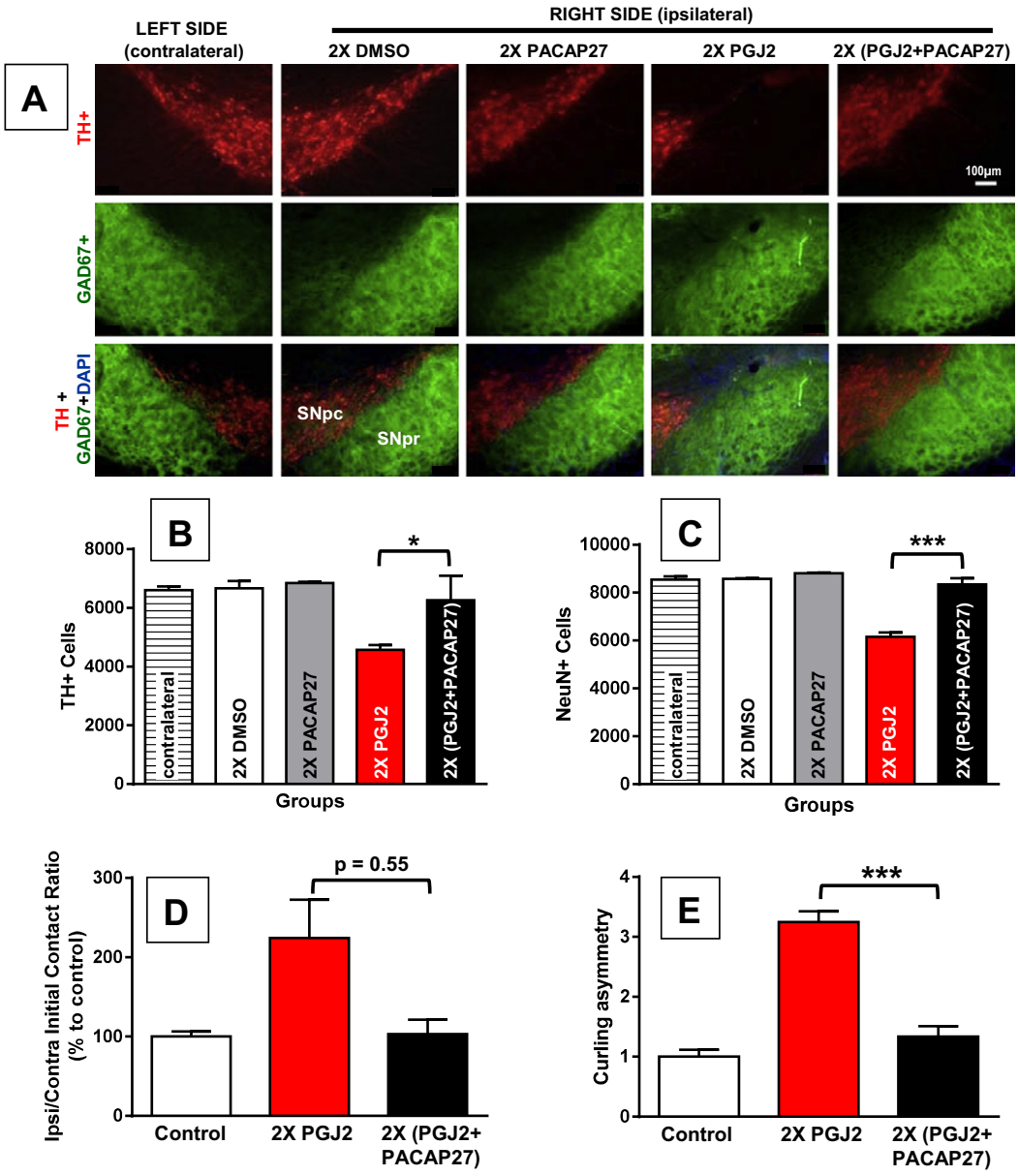

Fig. 7. PACAP27 prevents dopaminergic cell loss and behavior deficits induced by repeated PGJ2 microinfusion. A and B — TH+, and C — NeuN + immunoreactivity decreased in the ipsilateral SNpc of mice receiving two (2×) PGJ2 injections. GABAergic neurons in the SN *pars reticulata* were spared. Scale bar = 100 µm. D and E — Mice treated 2× with PGJ2 significantly increased usage of the ipsilateral forepaw as measured by the cylinder test (D), and exhibited significant postural instability assessed with the curling test (E) as described in Materials and methods ($N = 3$ to 6 mice per group). Co-injection with PACAP27 prevented neuronal loss (A–C) and behavioral deficits (D and E), induced by successive PGJ2 injections. The extent of PGJ2 lesion was assessed by calculating the total number of TH + (B) or NeuN + (C) neurons in the SNpc using unbiased stereology as described in Materials and methods ($N = 3$ to 4 mice per group). The asterisk (*) identifies the values that are significantly different: *, $p < 0.05$; ***, $p < 0.001$. In mice treated with DMSO or PACAP27 alone, the values obtained for the immunohistochemical analyses of contralateral and ipsilateral SNpc as well as behavioral analyses, were not significantly different.

DP2 receptor, decreasing cAMP levels [28,59] and potentiating neuronal injury [28,49]. On the other hand, PGJ2 and its metabolites have a cyclopentenone ring with reactive α,β-unsaturated carbonyl groups that form covalent Michael adducts with free sulfhydryls in cysteine residues in glutathione and cellular proteins [80,87]. Endogenous compounds such as PGJ2 that forms covalent bonds with proteins through electrophilic attack on side chains, such as that of the sulfhydryl group of cysteine, are regarded as playing an important role in determining whether neurons will live or die [74]. The covalent protein modification by PGJ2 in the brain represents a novel pathologic post-translational change and could play a critical role in neurodegeneration in PD [32].

To overcome the PGJ2-induced deficits we tested PACAP27 as it provides DA neuroprotection in models of PD [71]. Furthermore, PACAP has a relative low molecular weight, is lipophilic, and crosses the blood–brain barrier [20]. The simultaneous administration of PGJ2 with PACAP27 had two contrasting outcomes. On the one hand, it significantly reduced the level of DA neuronal loss in the SN as well as the behavioral motor deficits. On the other hand, it failed to prevent the accumulation/aggregation of neuronal ubiquitinated proteins as well as microglia activation. These in vivo studies provide the proof-of-principle that PACAP27 has potential as a therapeutic strategy to target mechanisms leading to neuronal loss assessed by TH staining and associated motor deficits, but not for mechanisms controlling ubiquitin-protein accumulation/aggregation or microglia activation. In the previous in vitro studies with neuronal cultures we also observed that PACAP27 failed to diminish the accumulation/aggregation of ubiquitinated proteins induced by PGJ2 [57].

PACAP27 binds to a range of receptors at various concentrations and activates a variety of second messengers that are dependent not only on the receptor and G-proteins but also on a repertoire of accessory

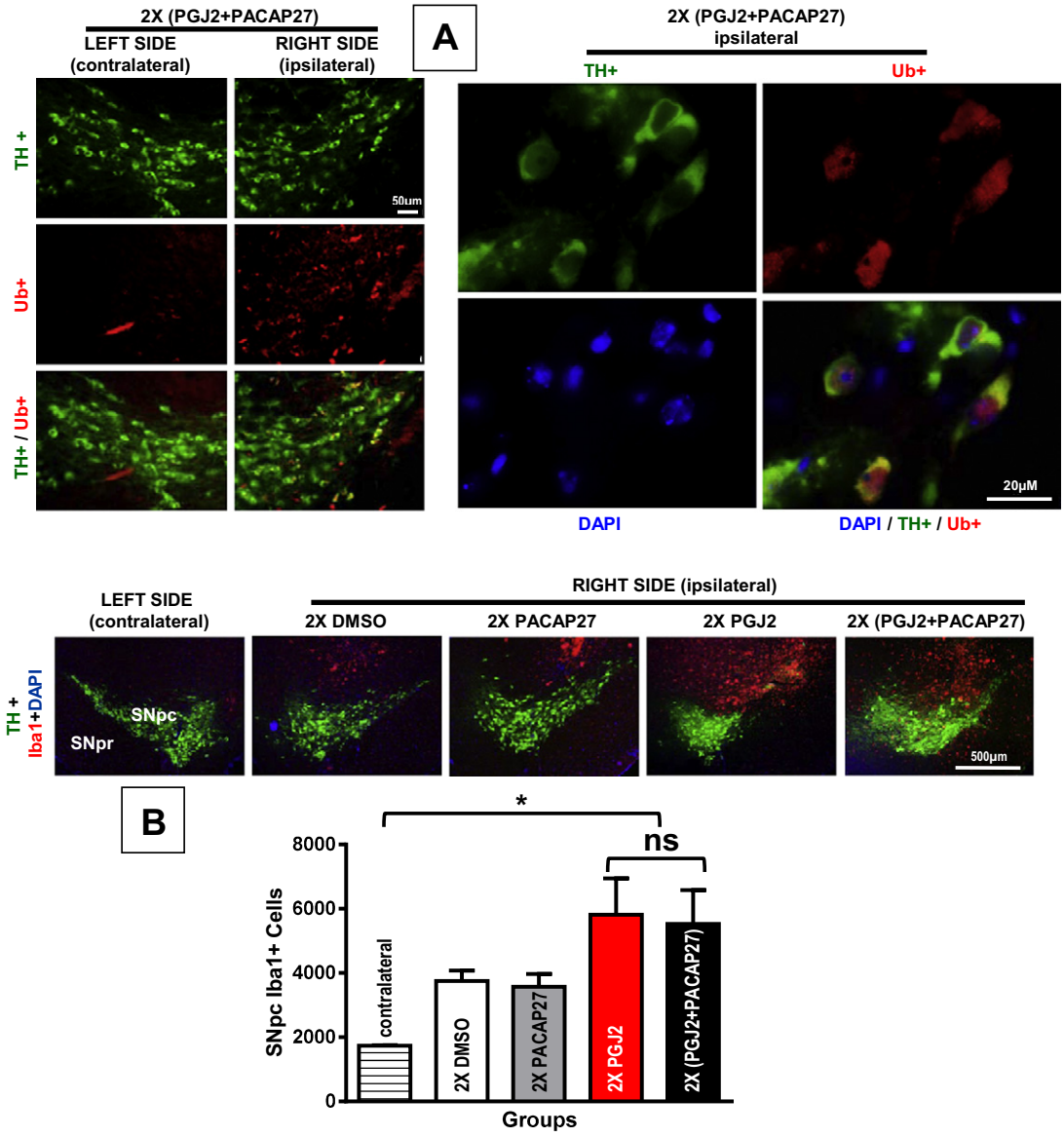

Fig. 8. PACAP27 does not prevent PGJ2-induced accumulation/aggregation of ubiquitinated proteins or microglia activation. A — In mice receiving two (2×) (PGJ2 + PACAP27) injections, the accumulation/aggregation of ubiquitinated proteins (Ub; *red*) was more prevalent in the ipsilateral than in the contralateral SNpc, while TH + immunoreactivity (*green*) in both sides was similar. Scale bar = 50 μm (left panels), 20 μm (right panels, high magnification). B — In mice treated with 2× PGJ2 alone or combined with PACAP27, the number of Iba1 + cells (*red*) in the ipsilateral SNpc was similar (ns, not significantly different), but higher than that in the contralateral SNpc (*, $p < 0.05$). The total number of Iba1 + cells in the SNpc, which depicts activated microglia, was assessed with unbiased stereology as described in Materials and methods ($N = 3$ to 4 mice per group).

molecules [82]. We plan to address PACAP signaling pathways in our PGJ2-induced mouse model in the future studies, but one of the pathways by which PACAP signals survival is via activation of the G-protein coupled receptor PAC1R (pituitary adenylate cyclase 1 receptor). We previously showed in vitro, that PGJ2 lowers neuronal cAMP while PACAP raises neuronal cAMP [57]. In addition, PACAP27 prevented some but not all of the neurotoxic effects of PGJ2 [57]. There are several factors that could contribute to the lack of protection by PACAP27. In regard to the ubiquitinated proteins, PGJ2 impairs the UPP by targeting different components of this pathway including (a) the 26S proteasome by perturbing its assembly [65,90] and oxidatively modifying the S6ATPase (Rpt3) subunit [37], (b) inhibiting de-ubiquitinating enzymes [41,47,50,61], and (c) causing the accumulation/aggregation of ubiquitinated (Ub) proteins [51]. It is likely that PACAP27 can override the negative effect of PGJ2 on the proteasome because several components of the UPP are up-regulated by the activation of the cAMP signaling [34], including proteasome subunits, thus leading to an increase in proteasome activity [62]. However, PACAP27 may be unable to protect UPP components such as UCH-L1 and other de-ubiquitinating enzymes, which are covalently modified at specific cysteine residues by PGJ2 [41,61].

The finding that PACAP27 failed to prevent microglia activation induced by PGJ2 could be attributed to a mechanism supported by animal studies, in that besides being mediators of acute inflammation, prostaglandins also function in the transition and maintenance of chronic inflammation, thus inducing long-lasting effects [3] that may be refractory to short-term rises in cAMP levels. Persistent Ub-aggregates and microglia activation could eventually exert deleterious effects on neurons and behavior. It is known that individuals that suffer mild brain injuries early in life, may exhibit pathology at a much older age. Our model would be ideal to address the potential long term effects of persistent protein accumulation/aggregation and chronic inflammation in the aging brain.

In conclusion, we demonstrate that consecutive infusions of PGJ2 into the *substantia nigra* of mice to mimic in part chronic inflammation,

induce a slow-onset of Parkinsonian-like neuronal and motor deficits, as well as microglia activation. The latter can be imaged in vivo by μPET with [^{11}C](R)PK11195. We also show that the protection by PACAP27 observed over the short term (two weeks) was sufficient to prevent neuronal loss and behavioral deficits induced by PGJ2, while microglia activation persisted. If not halted, the latter could lead to chronic inflammation with long-term effects resulting in gradual neurodegeneration, like in PD. Developing successful anti-inflammatory drugs that potentially target prostaglandin signaling downstream of COX-2, could be accelerated by non-invasive molecular imaging techniques, such as PET, that can monitor regional responses in order to effectively assess early remediation therapies designed to provide overall neuronal and glial benefits for patients with PD.

Acknowledgements

The authors thank Dalila Ordonez, Carolyn Diaz, Vanessa Jacob (Hunter College), Michael Synan and Dr. Bin He (Weill Cornell Medical College) for their excellent technical assistance. Supported by NIH: AG028847/NIA to M.F.-P.; and NS041073/NINDS (SNRP) to M.F.-P. (head of subproject); CTSC GRANT UL1-RR024996 (TL1 training award to K.-Y.S.); and MD007599/NIMHD/RCMI to Hunter College; and Training Program at Hunter College (BP-Endure Grant 1R25GM097634 to S.I.M.). The authors declare no competing financial interests.

References

[1] M.S. Abdel-Halim, M. Hamberg, B. Sjoquist, E. Anggard, Identification of prostaglandin D2 as a major prostaglandin in homogenates of rat brain, Prostaglandins 14 (1977) 633–643.
[2] P. Anglade, A. Mouatt-Prigent, Y. Agid, E. Hirsch, Synaptic plasticity in the caudate nucleus of patients with Parkinson's disease, Neurodegeneration 5 (1996) 121–128.
[3] T. Aoki, S. Narumiya, Prostaglandins and chronic inflammation, Trends Pharmacol. Sci. 33 (2012) 304–311.
[4] T. Atlasz, K. Szabadfi, P. Kiss, A. Tamas, G. Toth, D. Reglodi, R. Gabriel, Evaluation of the protective effects of PACAP with cell-specific markers in ischemia-induced retinal degeneration, Brain Res. Bull. 81 (2010) 497–504.
[5] R.B. Banati, Visualising microglial activation in vivo, Glia 40 (2002) 206–217.
[6] Z.C. Baquet, D. Williams, J. Brody, R.J. Smeyne, A comparison of model-based (2D) and design-based (3D) stereological methods for estimating cell number in the substantia nigra pars compacta (SNpc) of the C57BL/6J mouse, Neuroscience 161 (2009) 1082–1090.
[7] A.L. Bartels, K.L. Leenders, Cyclooxygenase and neuroinflammation in Parkinson's disease neurodegeneration, Curr. Neuropharmacol. 8 (2010) 62–68.
[8] C. Becker, S.S. Jick, C.R. Meier, Risk of stroke in patients with idiopathic Parkinson disease, Parkinsonism Relat. Disord. 16 (2010) 31–35.
[9] H. Bernheimer, W. Birkmayer, O. Hornykiewicz, K. Jellinger, F. Seitelberger, Brain dopamine and the syndromes of Parkinson and Huntington. Clinical, morphological and neurochemical correlations, J. Neurol. Sci. 20 (1973) 415–455.
[10] R. Betarbet, O. Poisik, T.B. Sherer, J.T. Greenamyre, Differential expression and ser897 phosphorylation of striatal N-methyl-d-aspartate receptor subunit NR1 in animal models of Parkinson's disease, Exp. Neurol. 187 (2004) 76–85.
[11] P. Calabresi, B. Picconi, A. Tozzi, F.M. Di, Dopamine-mediated regulation of corticostriatal synaptic plasticity, Trends Neurosci. 30 (2007) 211–219.
[12] M.M. Carvalho, F.L. Campos, B. Coimbra, J.M. Pego, C. Rodrigues, R. Lima, A.J. Rodrigues, N. Sousa, A.J. Salgado, Behavioral characterization of the 6-hydroxidopamine model of Parkinson's disease and pharmacological rescuing of non-motor deficits, Mol. Neurodegener. 8 (2013) 14.
[13] A.S. Ching, B. Kuhnast, A. Damont, D. Roeda, B. Tavitian, F. Dolle, Current paradigm of the 18-kDa translocator protein (TSPO) as a molecular target for PET imaging in neuroinflammation and neurodegenerative diseases, Insights Imaging 3 (2012) 111–119.
[14] E.K. Chiu, J.S. Richardson, Behavioral and neurochemical aspects of prostaglandins in brain function, Gen. Pharmacol. 16 (1985) 163–175.
[15] H.M. Cox, Pituitary adenylate cyclase activating polypeptides, PACAP-27 and PACAP-38: stimulators of electrogenic ion secretion in the rat small intestine, Br. J. Pharmacol. 106 (1992) 498–502.
[16] M. Day, Z. Wang, J. Ding, X. An, C.A. Ingham, A.F. Shering, D. Wokosin, E. Ilijic, Z. Sun, A.R. Sampson, E. Mugnaini, A.Y. Deutch, S.R. Sesack, G.W. Arbuthnott, D.J. Surmeier, Selective elimination of glutamatergic synapses on striatopallidal neurons in Parkinson disease models, Nat. Neurosci. 9 (2006) 251–259.
[17] J. Deguil, F. Chavant, C. Lafay-Chebassier, M.C. Perault-Pochat, B. Fauconneau, S. Pain, Neuroprotective effect of PACAP on translational control alteration and cognitive decline in MPTP parkinsonian mice, Neurotox. Res. 17 (2010) 142–155.
[18] A. Dejda, T. Seaborn, S. Bourgault, O. Touzani, A. Fournier, H. Vaudry, D. Vaudry, PACAP and a novel stable analog protect rat brain from ischemia: Insight into the mechanisms of action, Peptides 32 (2011) 1207–1216.
[19] M. Deleidi, T. Gasser, The role of inflammation in sporadic and familial Parkinson's disease, Cell. Mol. Life Sci. 70 (20) (2013 Nov) 4259–4273.
[20] D. Dogrukol-Ak, F. Tore, N. Tuncel, Passage of VIP/PACAP/secretin family across the blood–brain barrier: therapeutic effects, Curr. Pharm. Des. 10 (2004) 1325–1340.
[21] D. Ebrahimi-Fakhari, L. Wahlster, P.J. McLean, Protein degradation pathways in Parkinson's disease: curse or blessing, Acta Neuropathol. 124 (2012) 153–172.
[22] E. Esposito, V. Di M., A. Benigno, M. Pierucci, G. Crescimanno, G.G. Di, Non-steroidal anti-inflammatory drugs in Parkinson's disease, Exp. Neurol. 205 (2007 Jun) 295–312 Epub 2007 Feb 23.
[23] S. Fahn, L.R. Libsch, R.W. Cutler, Monoamines in the human neostriatum: topographic distribution in normals and in Parkinson's disease and their role in akinesia, rigidity, chorea, and tremor, J. Neurol. Sci. 14 (1971) 427–455.
[24] J.M. Fearnley, A.J. Lees, Ageing and Parkinson's disease: substantia nigra regional selectivity, Brain 114 (Pt 5) (1991) 2283–2301.
[25] Z. Feng, D. Li, P.C. Fung, Z. Pei, D.B. Ramsden, S.L. Ho, COX-2-deficient mice are less prone to MPTP-neurotoxicity than wild-type mice, Neuroreport 14 (2003) 1927–1929.
[26] M.Y. Golovko, E.J. Murphy, Brain prostaglandin formation is increased by alpha-synuclein gene-ablation during global ischemia, Neurosci. Lett. 432 (2008) 243–247.
[27] S. Grealish, B. Mattsson, P. Draxler, A. Bjorklund, Characterisation of behavioural and neurodegenerative changes induced by intranigral 6-hydroxydopamine lesions in a mouse model of Parkinson's disease, Eur. J. Neurosci. 31 (2010) 2266–2278.
[28] A.N. Hata, R. Zent, M.D. Breyer, R.M. Breyer, Expression and molecular pharmacology of the mouse CRTH2 receptor, J. Pharmacol. Exp. Ther. 306 (2003) 463–470.
[29] J.M. Henderson, L.E. Annett, L.J. Ryan, W. Chiang, S. Hidaka, E.M. Torres, S.B. Dunnett, Subthalamic nucleus lesions induce deficits as well as benefits in the hemiparkinsonian rat, Eur. J. Neurosci. 11 (1999) 2749–2757.
[30] J.L. Herlong, T.R. Scott, Positioning prostanoids of the D and J series in the immunopathogenic scheme, Immunol. Lett. 102 (2006) 121–131.
[31] R.W. Hickey, P.D. Adelson, M.J. Johnnides, D.S. Davis, Z. Yu, M.E. Rose, Y.F. Chang, S.H. Graham, Cyclooxygenase-2 activity following traumatic brain injury in the developing rat, Pediatr. Res. 62 (2007) 271–276.
[32] A.N. Higdon, A. Landar, S. Barnes, V.M. Darley-Usmar, The electrophile responsive proteome: integrating proteomics and lipidomics with cellular function, Antioxid. Redox Signal. 17 (2012) 1580–1589.
[33] E. Hirsch, A.M. Graybiel, Y.A. Agid, Melanized dopaminergic neurons are differentially susceptible to degeneration in Parkinson's disease, Nature 334 (1988) 345–348.
[34] H. Huang, H. Wang, M.E. Figueiredo-Pereira, Regulating the ubiquitin/proteasome pathway via cAMP-signaling: neuroprotective potential, Cell Biochem. Biophys. 67 (2013) 55–66.
[35] C.B. Hutson, C.R. Lazo, F. Mortazavi, C.C. Giza, D. Hovda, M.F. Chesselet, Traumatic brain injury in adult rats causes progressive nigrostriatal dopaminergic cell loss and enhanced vulnerability to the pesticide paraquat, J. Neurotrauma 28 (2011) 1783–1801.
[36] C. Iadecola, P.B. Gorelick, The Janus face of cyclooxygenase-2 in ischemic stroke: shifting toward downstream targets, Stroke 36 (2005) 182–185.
[37] T. Ishii, T. Sakurai, H. Usami, K. Uchida, Oxidative modification of proteasome: identification of an oxidation-sensitive subunit in 26s proteasome, Biochemistry 44 (2005) 13893–13901.
[38] K.M. Joo, Y.H. Chung, M.K. Kim, R.H. Nam, B.L. Lee, K.H. Lee, C.I. Cha, Distribution of vasoactive intestinal peptide and pituitary adenylate cyclase-activating polypeptide receptors (VPAC1, VPAC2, and PAC1 receptor) in the rat brain, J. Comp. Neurol. 476 (2004) 388–413.
[39] K. Kierdorf, M. Prinz, Factors regulating microglia activation, Front. Cell. Neurosci. 7 (2013) 44.
[40] P. Klivenyi, G. Gardian, N.Y. Calingasan, L. Yang, M.F. Beal, Additive neuroprotective effects of creatine and a cyclooxygenase 2 inhibitor against dopamine depletion in the 1-methyl-4-phenyl-1,2,3,6-tetrahydropyridine (MPTP) mouse model of Parkinson's disease, J. Mol. Neurosci. 21 (2003) 191–198.
[41] L.M. Koharudin, H. Liu, M.R. Di, R.B. Kodali, S.H. Graham, A.M. Gronenborn, Cyclopentenone prostaglandin-induced unfolding and aggregation of the Parkinson disease-associated UCH-L1, Proc. Natl. Acad. Sci. U. S. A. 107 (2010) 6835–6840.
[42] M. Kondo, T. Oya-Ito, T. Kumagai, T. Osawa, K. Uchida, Cyclopentenone prostaglandins as potential inducers of intracellular oxidative stress, J. Biol. Chem. 276 (2001) 12076–12083.
[43] M. Kondo, T. Shibata, T. Kumagai, T. Osawa, N. Shibata, M. Kobayashi, S. Sasaki, M. Iwata, N. Noguchi, K. Uchida, 15-Deoxy-delta(12,14)-prostaglandin J(2): the endogenous electrophile that induces neuronal apoptosis, Proc. Natl. Acad. Sci. U. S. A. 99 (2002) 7367–7372.
[44] J.B. Koprich, C. Reske-Nielsen, P. Mithal, O. Isacson, Neuroinflammation mediated by IL-1beta increases susceptibility of dopamine neurons to degeneration in an animal model of Parkinson's disease, J. Neuroinflammation 5 (2008) 8.
[45] T. Kunz, N. Marklund, L. Hillered, E.H. Oliw, Cyclooxygenase-2, prostaglandin synthases, and prostaglandin H2 metabolism in traumatic brain injury in the rat, J. Neurotrauma 19 (2002) 1051–1064.
[46] Z. Li, M. Jansen, K. Ogburn, L. Salvatierra, L. Hunter, S. Mathew, M.E. Figueiredo-Pereira, Neurotoxic prostaglandin J2 enhances cyclooxygenase-2 expression in neuronal cells through the p38MAPK pathway: a death wish? J. Neurosci. Res. 78 (2004) 824–836.
[47] Z. Li, F. Melandri, I. Berdo, M. Jansen, L. Hunter, S. Wright, D. Valbrun, M.E. Figueiredo-Pereira, Delta12-Prostaglandin J2 inhibits the ubiquitin hydrolase UCH-L1 and elicits ubiquitin-protein aggregation without proteasome inhibition, Biochem. Biophys. Res. Commun. 319 (2004) 1171–1180.
[48] X. Liang, L. Wu, T. Hand, K. Andreasson, Prostaglandin D2 mediates neuronal protection via the DP1 receptor, J. Neurochem. 92 (2005) 477–486.
[49] X. Liang, L. Wu, Q. Wang, T. Hand, M. Bilak, L. McCullough, K. Andreasson, Function of COX-2 and prostaglandins in neurological disease, J. Mol. Neurosci. 33 (2007) 94–99.

[50] H. Liu, W. Li, M. Ahmad, T.M. Miller, M.E. Rose, S.M. Poloyac, G. Uechi, M. Balasubramani, R.W. Hickey, S.H. Graham, Modification of ubiquitin-C-terminal hydrolase-L1 by cyclopentenone prostaglandins exacerbates hypoxic injury, Neurobiol. Dis. 41 (2011) 318–328.
[51] H. Liu, W. Li, M. Ahmad, M.E. Rose, T.M. Miller, M. Yu, J. Chen, J.L. Pascoe, S.M. Poloyac, R.W. Hickey, S.H. Graham, Increased generation of cyclopentenone prostaglandins after brain ischemia and their role in aggregation of ubiquitinated proteins in neurons, Neurotox. Res. 24 (2013) 191–204.
[52] H. Liu, W. Li, M.E. Rose, J.L. Pascoe, T.M. Miller, M. Ahmad, S.M. Poloyac, R.W. Hickey, S.H. Graham, Prostaglandin D toxicity in primary neurons is mediated through its bioactive cyclopentenone metabolites, Neurotoxicology 39C (2013) 35–44.
[53] S.S. Mao, R. Hua, X.P. Zhao, X. Qin, Z.Q. Sun, Y. Zhang, Y.Q. Wu, M.X. Jia, J.L. Cao, Y.M. Zhang, Exogenous administration of PACAP alleviates traumatic brain injury in rats through a mechanism involving the TLR4/MyD88/NF-kappaB pathway, J. Neurotrauma 29 (2012) 1941–1959.
[54] B. Martinez, A. Perez-Castillo, A. Santos, The mitochondrial respiratory complex I is a target for 15-deoxy-delta12,14-prostaglandin J2 action, J. Lipid Res. 46 (2005) 736–743.
[55] E.G. McGeer, P.L. McGeer, The role of anti-inflammatory agents in Parkinson's disease, CNS Drugs 21 (2007) 789–797.
[56] G.E. Meredith, U.J. Kang, Behavioral models of Parkinson's disease in rodents: a new look at an old problem, Mov. Disord. 21 (2006) 1595–1606.
[57] M.J. Metcalfe, Q. Huang, M.E. Figueiredo-Pereira, Coordination between proteasome impairment and caspase activation leading to TAU pathology: neuroprotection by cAMP, Cell Death Dis. 3 (2012) e326.
[58] M. Mogi, M. Harada, T. Kondo, P. Riederer, H. Inagaki, M. Minami, T. Nagatsu, Interleukin-1 beta, interleukin-6, epidermal growth factor and transforming growth factor-alpha are elevated in the brain from parkinsonian patients, Neurosci. Lett. 180 (1994) 147–150.
[59] G. Monneret, H. Li, J. Vasilescu, J. Rokach, W.S. Powell, 15-Deoxy-delta 12,14-prostaglandins D2 and J2 are potent activators of human eosinophils, J. Immunol. 168 (2002) 3563–3569.
[60] T.W. Moody, T. Ito, N. Osefo, R.T. Jensen, VIP and PACAP: recent insights into their functions/roles in physiology and disease from molecular and genetic studies, Curr. Opin. Endocrinol. Diabetes Obes. 18 (2011) 61–67.
[61] J.E. Mullally, P.J. Moos, K. Edes, F.A. Fitzpatrick, Cyclopentenone prostaglandins of the J series inhibit the ubiquitin isopeptidase activity of the proteasome pathway, J. Biol. Chem. 276 (2001) 30366–30373.
[62] N. Myeku, H. Wang, M.E. Figueiredo-Pereira, cAMP stimulates the ubiquitin/proteasome pathway in rat spinal cord neurons, Neurosci. Lett. 527 (2012) 126–131.
[63] E.L. Nelson, C.L. Liang, C.M. Sinton, D.C. German, Midbrain dopaminergic neurons in the mouse: computer-assisted mapping, J. Comp. Neurol. 369 (1996) 361–371.
[64] K.D. Ogburn, T. Bottiglieri, Z. Wang, M.E. Figueiredo-Pereira, Prostaglandin J2 reduces catechol-O-methyltransferase activity and enhances dopamine toxicity in neuronal cells, Neurobiol. Dis. 22 (2006) 294–301.
[65] K.D. Ogburn, M.E. Figueiredo-Pereira, Cytoskeleton/endoplasmic reticulum collapse induced by prostaglandin J2 parallels centrosomal deposition of ubiquitinated protein aggregates, J. Biol. Chem. 281 (2006) 23274–23284.
[66] H. Ohtaki, A. Satoh, T. Nakamachi, S. Yofu, K. Dohi, H. Mori, K. Ohara, K. Miyamoto, H. Hashimoto, N. Shintani, A. Baba, M. Matsunaga, S. Shioda, Regulation of oxidative stress by pituitary adenylate cyclase-activating polypeptide (PACAP) mediated by PACAP receptor, J. Mol. Neurosci. 42 (2010) 397–403.
[67] G. Paxinos, K.B.J. Franklin, The Mouse Brain in Stereotaxic Coordinates, Academic, San Diego, 2001.
[68] B. Picconi, F. Gardoni, D. Centonze, D. Mauceri, M.A. Cenci, G. Bernardi, P. Calabresi, L. M. Di, Abnormal Ca2 + -calmodulin-dependent protein kinase II function mediates synaptic and motor deficits in experimental parkinsonism, J. Neurosci. 24 (2004) 5283–5291.
[69] S.R. Pierre, M.A. Lemmens, M.E. Figueiredo-Pereira, Subchronic infusion of the product of inflammation prostaglandin J2 models sporadic Parkinson's disease in mice, J. Neuroinflammation 6 (2009) 18.
[70] M.C. Pott Godoy, R. Tarelli, C.C. Ferrari, M.I. Sarchi, F.J. Pitossi, Central and systemic IL-1 exacerbates neurodegeneration and motor symptoms in a model of Parkinson's disease, Brain 131 (2008) 1880–1894.
[71] D. Reglodi, P. Kiss, A. Lubics, A. Tamas, Review on the protective effects of PACAP in models of neurodegenerative diseases in vitro and in vivo, Curr. Pharm. Des. 17 (2011) 962–972.
[72] D. Reglodi, A. Lubics, A. Tamas, L. Szalontay, I. Lengvari, Pituitary adenylate cyclase activating polypeptide protects dopaminergic neurons and improves behavioral deficits in a rat model of Parkinson's disease, Behav. Brain Res. 151 (2004) 303–312.
[73] B. Rodriguez-Grande, V. Blackabey, B. Gittens, E. Pinteaux, A. Denes, Loss of substance P and inflammation precede delayed neurodegeneration in the substantia nigra after cerebral ischemia, Brain Behav. Immun. 29 (2013) 51–61.
[74] T. Satoh, S.A. Lipton, Redox regulation of neuronal survival mediated by electrophilic compounds, Trends Neurosci. 30 (2007) 37–45.
[75] T. Schallert, S.M. Fleming, J.L. Leasure, J.L. Tillerson, S.T. Bland, CNS plasticity and assessment of forelimb sensorimotor outcome in unilateral rat models of stroke, cortical ablation, parkinsonism and spinal cord injury, Neuropharmacology 39 (2000) 777–787.
[76] T. Shibata, T. Yamada, M. Kondo, N. Tanahashi, K. Tanaka, H. Nakamura, H. Masutani, J. Yodoi, K. Uchida, An endogenous electrophile that modulates the regulatory mechanism of protein turnover: inhibitory effects of 15-deoxy-delta(12,14)-prostaglandin J2 on proteasome, Biochemistry 42 (2003) 13960–13968.
[77] A.Y. Shih, H.B. Fernandes, F.Y. Choi, M.G. Kozoriz, Y. Liu, P. Li, C.M. Cowan, A. Klegeris, Policing the police: astrocytes modulate microglial activation, J. Neurosci. 26 (2006) 3887–3888.
[78] M.S. Silveira, R. Linden, Neuroprotection by cAMP: another brick in the wall, Adv. Exp. Med. Biol. 557 (2006) 164–176.
[79] N. Sousa, O.F. Almeida, C.T. Wotjak, A hitchhiker's guide to behavioral analysis in laboratory rodents, Genes Brain Behav. 5 (Suppl. 2) (2006) 5–24.
[80] D.S. Straus, C.K. Glass, Cyclopentenone prostaglandins: new insights on biological activities and cellular targets, Med. Res. Rev. 21 (2001) 185–210.
[81] N. Takei, Y. Skoglosa, D. Lindholm, Neurotrophic and neuroprotective effects of pituitary adenylate cyclase-activating polypeptide (PACAP) on mesencephalic dopaminergic neurons, J. Neurosci. Res. 54 (1998) 698–706.
[82] Y.V. Tan, J.A. Waschek, Targeting VIP and PACAP receptor signalling: new therapeutic strategies in multiple sclerosis, ASN Neuro 3 (2011) (p.pii:e00065).
[83] S. Tanaka, A. Ishii, H. Ohtaki, S. Shioda, T. Yoshida, S. Numazawa, Activation of microglia induces symptoms of Parkinson's disease in wild-type, but not in IL-1 knockout mice, J. Neuroinflammation 10 (2013) 143.
[84] M.G. Tansey, M.S. Goldberg, Neuroinflammation in Parkinson's disease: its role in neuronal death and implications for therapeutic intervention, Neurobiol. Dis. 37 (2010) 510–518.
[85] P. Teismann, K. Tieu, D.K. Choi, D.C. Wu, A. Naini, S. Hunot, M. Vila, V. Jackson-Lewis, S. Przedborski, Cyclooxygenase-2 is instrumental in Parkinson's disease neurodegeneration, Proc. Natl. Acad. Sci. U. S. A. 100 (2003) 5473–5478.
[86] H. Uchida, H. Yokoyama, H. Kimoto, H. Kato, T. Araki, Long-term changes in the ipsilateral substantia nigra after transient focal cerebral ischaemia in rats, Int. J. Exp. Pathol. 91 (2010) 256–266.
[87] K. Uchida, T. Shibata, 15-Deoxy-delta(12,14)-prostaglandin J2: an electrophilic trigger of cellular responses, Chem. Res. Toxicol. 21 (2008) 138–144.
[88] S. Venneti, B.J. Lopresti, C.A. Wiley, Molecular imaging of microglia/macrophages in the brain, Glia 61 (2013) 10–23.
[89] G. Wang, J. Pan, Y.Y. Tan, X.K. Sun, Y.F. Zhang, H.Y. Zhou, R.J. Ren, X.J. Wang, S.D. Chen, Neuroprotective effects of PACAP27 in mice model of Parkinson's disease involved in the modulation of K(ATP) subunits and D2 receptors in the striatum, Neuropeptides 42 (2008) 267–276.
[90] Z. Wang, V.M. Aris, K.D. Ogburn, P. Soteropoulos, M.E. Figueiredo-Pereira, Prostaglandin J2 alters pro-survival and pro-death gene expression patterns and 26S proteasome assembly in human neuroblastoma cells, J. Biol. Chem. 281 (2006) 21377–21386.
[91] S.T. Warraich, H.N. Allbutt, R. Billing, J. Radford, M.J. Coster, M. Kassiou, J.M. Henderson, Evaluation of behavioural effects of a selective NMDA NR1A/2B receptor antagonist in the unilateral 6-OHDA lesion rat model, Brain Res. Bull. 78 (2009) 85–90.
[92] M.B. Watson, H. Nobuta, C. Abad, S.K. Lee, N. Bala, C. Zhu, F. Richter, M.F. Chesselet, J. A. Waschek, PACAP deficiency sensitizes nigrostriatal dopaminergic neurons to paraquat-induced damage and modulates central and peripheral inflammatory activation in mice, Neuroscience 240 (2013) 277–286.